Molecular Modeling Connect
ISSN: 3006-9084
2025, Article ID. 2025.0010, Cite as: https://doi.org/10.69709/MolModC.2025.112309

SCIFINITI

Research Article

OPEN ACCESS

Structural and Molecular Changes of Isonicotinylhydrazine Anti-Tubercular Drug in Alcohol Environment: An Intuition from Theory

Chinyere A. Anyama[✉,1,*], **Emmanuel A. Anyama**[✉,2] and **Ayi A. Ayi**[✉,1]

[1] Department of Pure and Applied Chemistry, University of Calabar, Calabar 540242, Cross River State, Nigeria
[2] Department of Pharmacology, University of Calabar, Calabar 540242, Cross River State, Nigeria

Article History
Submitted: March 11, 2025 Accepted: July 10, 2025 Published: July 25, 2025

Abstract
Isonicotinylhydrazine (INH), also known as isoniazid, was attached with an alcohol active group at C1, C2, C4, C5, and N atoms to form INHOH1, INHOH2, INHOH4, INHOH5, and INHOHN molecules. From our result, we observed that the absorption wavelength of INH was extended remarkably, 295 nm and 547 nm in INHOH2 and INHOHN, respectively. C=C stretching vibrations were observed at 1604.88 cm^{-1}, 1618.98 cm^{-1}, 1601.69 cm^{-1}, 1607.23 cm^{-1}, 1621.00 cm^{-1} and 1652.89cm^{-1} for INH, INHOH1, INHOH2, INHOH4, INHOH5 and INHOHN respectively. NH_2 bending vibrations was observed at 1686.55 cm^{-1}, 1686.55 cm^{-1}, 1683.04cm^{-1}, 1688.49 cm^{-1}, 1685.26 cm^{-1} and 1676.35 cm^{-1} for INH, INHOH1, INHOH2, INHOH4, INHOH5 and INHOHN respectively. C=O stretching vibrations for INH were observed at 1778.91 cm^{-1} while for INHOH1, INHOH2, INHOH4, INHOH5 and INHOHN they were observed at 1777.07 cm^{-1}, 1732.58 cm^{-1}, 1769.27 cm^{-1}, 1781.81 cm^{-1}, 1732.57 cm^{-1}, respectively. Quantum chemical descriptors calculation shows that the interaction of the OH group with INH lowered the energy gap in all molecules, with the lowest energy gap (0.131 eV) observed for INHOHN, which suggests high interaction and reactivity. Natural bond orbital (NBO) analysis reveals that the transition from π*-π* had a major contribution to the electron transition. The positive binding energies calculated for the different molecules were 317.988 kcal/mol, 315.633 kcal/mol, 321.002 kcal/mol, 319.036 kcal/mol, and 2.0877 kcal/mol for INHOH1, INHOH2, INHOH4, INHOH5, and INHOHN, respectively. The positive binding energies indicate that alcohol binding to isoniazid is less favourable.

Keywords:
optimization; reactivity of INH; optical activities; binding energies; alcohol-medication interactions; electron transition

1. Introduction

Isonicotinylhydrazine (INH), also known as isoniazid, is an antibiotic used for the treatment of tuberculosis and other typical types of mycobacteria, such as Mycobacterium avium, Mycobacterium kansasii, and Mycobacterium xenopi [1–8]. The INH molecule has ligand properties that enable it to form complexes via its nitrogen and oxygen atoms. The NH_2 group exhibits electron-donating properties, while its nitrogen and oxygen atoms act as electron acceptors. Tuberculosis (TB) is known to contribute to a high percentage of deaths globally, which is attributed to its infectious nature. In 2016, an estimated 10.4 million cases of TB were reported, with approximately 4.7% associated with excessive alcohol use [9–12]. Alcohol misuse significantly hinders TB treatment, leading to severe health complications. Chronic alcoholics experience delayed culture conversion and are at higher risk of treatment failure, relapse, or even death [13–15]. Alcohol is an organic compound containing a hydroxyl (OH) group attached to an aliphatic carbon atom [16]. It belongs to the family of organics with the general molecular formulae ROH, where R is an alkyl group. The simplest members of the alcohol homologous series are methanol and ethanol. The hydroxyl group of alcohols differs from alkyl halides

* **Corresponding Author:**
Chinyere A. Anyama, Department of Pure and Applied Chemistry, University of Calabar, Calabar, Cross River State, Nigeria; anyamachinyere@unical.edu.ng

because it contains two reactive covalent bonds: the C–O bond and the O–H bond [16].

Oxygen (O) has higher electronegativity than carbon (C) and hydrogen (H), which leads to the polarized nature of the covalent bonds in the hydroxyl group, making oxygen electron-rich and both carbon and hydrogen electron-deficient [16]. The hydroxyl (OH) group is the most reactive site in an alcohol molecule, despite the fact that the O–H bond is stronger than the C–C, C–H, and C–O bonds, demonstrating that thermodynamic stability does not necessarily correlate with chemical reactivity [16]. In the human body, ethanol is metabolized into acetaldehyde by the action of alcohol dehydrogenase and then into acetic acid by the action of acetaldehyde dehydrogenase [17]. The first product of this metabolic process is acetaldehyde, which is more toxic than ethanol. Acetaldehyde is responsible for the majority of the clinical malfunctions of alcohol [17,18]. Alcohol-medication interactions are classified into pharmacokinetic and pharmacodynamic interactions [17]. Alcohol-medication pharmacokinetic interactions refer to alcohol induced changes in biological activities like absorption, distribution, metabolism, and excretion of a medication [18]. Alcohol-medication pharmacodynamic interactions are classified into two categories. One involves alcohol's pharmacodynamic effects on medications, referring to the influence of excessive or chronic alcohol use on a drug's binding site(s), altering its expected outcome [18]. The second category involves pharmacodynamic effects of the medication on alcohol, which refers to the effects of one-time or repeated use of a medication on alcohol at its binding site(s), modifying alcohol's mechanical and behavioural effects [16,17,19]. It is a common observation that antibiotic usage accompanied by alcohol consumption poses severe health consequences [20]. Patients who consume alcohol during treatment are at risk of experiencing disulfiram-like reactions. This has been reported for certain antibiotics, such as beta-lactams [21,22] and the cephalosporin ceftriaxone, with the latter occurring in very rare cases [23]. It is being reported that Isoniazid, an anti-tubercular drug, metabolizes rapidly in excessive alcoholic consumption, a situation leading to radical reduction in the overall performance of the drug [21]. Moreover, alcohol-isoniazid mixture is linked to isoniazid-related hepatotoxicity with the risk of disulfiram-like reactions [21,24]. Wendel and David (2012) reported clinical pharmacokinetics of isoniazid [25]. Ameeruddin et al. 2016 reported mechanisms of isoniazid action and resistance in mycobacterium tuberculosis [7]. Katiyar et al. reported a randomized controlled trial of high-dose isoniazid adjuvant therapy for multidrug-resistant tuberculosis [26]. Korarakin et al. studied the pharmacokinetics of isoniazid in patients with pulmonary tuberculosis and alcohol [27]. Lester reported the acetylation of isoniazid in alcohols [28]. Wilcke et al. reported unchanged acetylation of isoniazid by alcohol intake [29]. Anoop et al. reported a quantum chemical study of structural, electronic, and vibrational properties of isoniazid and its derivative [30]. Hajar and co-workers reported a Crystal Structure and Density Functional Theory Study on Structural Properties and Energies of an Isonicotinohydrazide Compound [31]. In all the reported studies on isoniazid, none have been directed towards the effect of alcohol on the structure and molecular properties of isoniazid. Here, we report the effect of alcohol on the structure, band-gap, optical properties, and reactivity of isoniazid. This could provide insights that may guide improved handling of drug disorders, enhance drug effectiveness, mitigate disulfiram-like reactions and hepatotoxicity associated with alcohol-isoniazid interactions, and inform better administration or modification of isoniazid, or the development of alternative drugs.

2. Computational Details

The molecular structure of isoniazid, an anti-tubercular drug extracted from literature, and its OH functionalized analogues were sketched with Gauss View 6.0 [32]. All calculations in this work were performed with the Gaussian 09W [33] package. Density functional theory (DFT) [34] with Becke's three-parameter exchange-functional combined with corrected correlation Lee, Yang, and Parr functional (B3LYP) [35,36] methods and 6-31+G (d,p) basis set were combined for geometry optimization at a minimum. Geometry optimization ensures that bond lengths and angles are adjusted to minimize the forces that pull atoms together or push them apart [37]. Plane or ordinary 6-31G basis set usually gives poor geometries when applied to molecules beyond the first row. This challenge can be addressed by introducing diffused (d) functions, called polarization functions, into the 6-31G basis set. The idea stems from the knowledge that the functions allow electronic distribution to be polarized along a specific direction [38]. Applying large basis sets with additional diffuse functions is critical for systems with large electron-nucleus distances. A typical example of a diffuse basis function is the 6-31+G (d, p) basis set, which was used in this work. The vibrational analysis was done at the same theory level, and optical performance in water was investigated with Time-dependent Self-Consistent Field (TD-SCF) and Integral Equation Formalism Polarized Continuum Model (IEF-PCM), which is useful in studying vibrational circular dichroism and molecular properties in solution. Natural bond orbital (NBO) version 3.1, which is embedded in the optimization file, was used to inves-

2025, Vol. 2, Article ID. 2025.0010
https://doi.org/10.69709/MolModC.2025.112309

tigate charge transfer patterns, bonding interactions, and electronic transitions.

3. Results and Discussion

3.1. Geometrical Parameters

The optimized structures, bond lengths, bond angles, and dihedral angles calculated using Gaussian 09 at B3LYP 6-31+G (d, p) are presented in Figure 1 and Tables 1–3. The results show that the geometrical parameters (bond lengths, bond angles, and dihedral angles) of INH were altered by the alcohol group, which could be the reason for the changes observed in its properties. C1-C2, which was calculated to be 1.394 Å in INH, was 1.403 Å, 1.412 Å, 1.391 Å, 1.392 Å, and 1.364 Å in INHOH1, INHOH2, INHOH4, INHOH5, and INHOHN, respectively. A similar trend was observed in the bond angles, where C1-C2-C3 (118.82°) for INH was calculated as 118.39°, 118.36°, 120.62°, 118.05°, and 121.45° for INHOH1, INHOH2, INHOH4, INHOH5, and INHOHN, respectively. C1-C2-C3-C10 was 179.40° for INH, and for INHOH1, INHOH2, INHOH4, INHOH5, and INHOHN, it was 179.9°, −178.58°, −179.99°, 179.37°, and −179.35°, respectively. The details of the changes in geometrical parameters are provided in the tables stated above.

3.2. Frontier Molecular Orbitals

The atomic orbital composition of the frontier molecular orbital for the studied molecules is shown in Figure 2. The frontier orbital, HOMO, and LUMO, determine the way the molecule interacts with other species. It is observed from the figure that HOMOs with high electron density are found to be close to the pyridyl ring nitrogen atom, the two ring carbon atoms meta to the nitrogen atom, and the secondary amine nitrogen atom. Whereas LUMOs are seen near all atoms except the primary amine nitrogen atom. The HOMO→LUMO transition shows that electrons were transferred to the aromatic part of the molecule. In the INHOH molecules, the HOMO orbitals, which are electron dense, are located near all the aromatic ring carbon atoms, the second-degree and third-degree amine nitrogen atoms, as well as the carbonyl oxygen atom. The LUMO orbitals are located at the second and third-degree amine nitrogen atoms, the carbon atoms of the aromatic ring where the cyano groups are attached, and the cyano nitrogen atoms. This shows that there is electronic interaction between the carbonyl oxygen atom and the aromatic ring directed towards the cyano nitrogen atoms, which represents HOMO→LUMO electronic transfers.

3.3. Quantum Chemical Descriptors

The energies of frontier molecular orbital (eHOMO, eLUMO), energy band gap (eHOMO - eLUMO), electronegativity (χ = (IP + EA)/2.), chemical potential (μ = −(IP + EA)/2), global hardness (η = (IP − EA)/2), global softness (S = 1/2η) and global electrophilicity index (ω = μ/2η) of the studied molecules were calculated using the famous Koopmans [39] equations above and results are presented in Table 4. Our result showed that the HOMO and LUMO energies were small, ranging from −0.26 and −0.16 and −0.07 and −0.03 eV, respectively, which highlights the existence of weak electron bonds in the molecules. Due to a small energy gap, rapid electron transfers and exchange occurred to the same degree, making these molecules very reactive. The energy gap for the studied molecules was observed in the following order: INHOHN (0.131 eV) < INHOH2 (0.171 eV) < INHOH1 (0.190 eV) < INHOH5 (0.191 eV) < INHOH4 (0.195 eV) < INH (0.198 eV). From our result, the interaction of alcohol with INH lowered its energy gap in all molecules, with the lowest energy gap (0.131 eV) observed in INH OHN, which shows that the highest change in reactivity of INH is when the OH group of alcohol attacks the nitrogen atom of the pyridyl ring. Lower kinetic stability is a function of a small energy gap due to the low activation energy of the system. Consequently, such molecules may experience adjustments in the charge density distribution via radical electron movements between the HOMO and LUMO orbitals and so react rapidly [40]. This could be the reason for the quick metabolism of INH in alcoholics and eventually decreased drug effectiveness. The calculated global quantum descriptors play a vital role in giving useful information about the electronic network and charge transfer behaviour of molecules. Chemical hardness (η) represents the resistance of atoms or atom groups to charge transfer [41]. From our results, alcohol lowered the resistance of INH to charge transfer. This could affect drug absorption and distribution, which is a major cause of treatment failure in INH—alcohol interaction. Electronegativity (χ) defines the ability of an atom group to attract electrons [42]. From our results, alcohol decreased the ability of INH to attract electrons, which could lead to delayed culture conversion. The measure of the ability of an atom or set of atoms to escape their ground/non-excited state is known as chemical potential (μ). It is an effective technique for studying molecules because it provides information about their solvation and transport properties. From our results, alcohol reduced the chemical potential of INH, which suggests that the ease of solvation and transport of INH may be hampered, which could be the reason for delayed absorption, distribution,

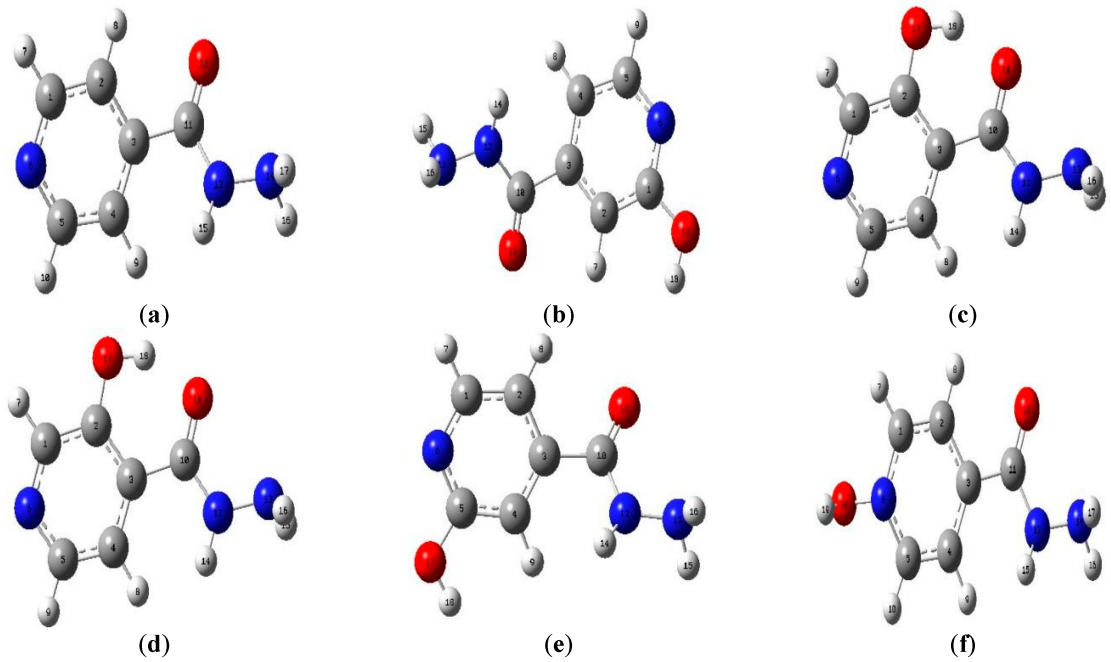

Figure 1: Optimized structures of INH (**a**), INH OH1 (**b**), INH OH2 (**c**), INH OH4 (**d**), INH OH5 (**e**), and INH OHN (**f**).

Table 1: Bond Length of Studied Molecules.

BONDLENGTH(Å)	INH	INH OH I	INH OH 2	INH OH 4	INH OH 5	INH OH N
C1-C2	1.394	1.403	1.412	1.391	1.392	1.364
C2-C3	1.398	1.392	1.414	1.401	1.400	1.429
C3-C4	1.400	1.403	1.407	1.404	1.396	1.425
C4-C5	1.397	1.394	1.388	1.401	1.406	1.367
C5-C6	1.338	1.338	1.346	1.331	1.326	1.394
C1-N6	1.345	1.329	1.326	1.341	1.341	1.399
C3-C11	1.511	1.512	1.494	1.522	1.510	1.478
C10--O11	1.220	1.220	1.288	1.222	1.219	1.228
C10-N12	1.378	1.376	1.367	1.369	1.380	1.396
N12-N13	1.397	1.397	1.397	1.400	1.392	1.402

Table 2: Bond Angles of Studied Molecules.

BOND ANGLES	INH	INH OH I	INH OH 2	INH OH 4	INH OH 5	INH OH N
C1-C2-C3	118.82	118.39	118.36	120.62	118.05	121.45
C2-C3-C4	117.84	118.50	116.86	115.98	118.53	116.42
C3-C4-C5	118.75	117.99	120.12	119.33	118.16	121.19
C1-N6-C5	117.08	117.33	117.96	117.15	117.43	118.63
C2-C1-N6	123.74	123.68	123.80	122.93	124.02	120.54
C2-C3-C11	118.13	117.21	118.13	115.91	118.46	118.20
C3-C11-O12	121.54	121.52	120.83	119.95	121.67	122.25
C3-C11-N13	114.05	114.07	116.96	115.89	113.81	114.98
C11-N13-N14	120.28	120.44	120.61	120.17	120.03	118.55
C4-C3-C11	123.99	124.27	125.00	128.09	122.87	125.29

and metabolism of INH in alcoholic patients. The electrophilicity index (ω) is a measure of a chemical species' ability to function as an electrophile, that is, to accept an electron pair from a nucleophile. From our result, the electrophilicity index of INH was increased in INHOH2, which means that its propensity to accept an electron pair

2025, Vol. 2, Article ID. 2025.0010
https://doi.org/10.69709/MolModC.2025.112309

Table 3: Dihedral Angles of Studied Molecules.

DIHEDRAL ANGLES	INH	INH OH I	INH OH 2	INH OH 4	INH OH 5	INH OH N
C1-C2-C3-C10	179.40	179.79	−178.58	−179.99	179.37	−179.35
C2-C3-C11-N13	151.54	153.73	172.71	−179.96	146.62	168.33
C3-C11-N12-N13	−179.19	−179.38	−179.86	179.99	−178.57	−178.23
C4-C3-C11-O12	149.66	152.83	172.92	−179.92	144.72	164.54
C5-C4-C3-C11	−178.75	−179.33	179.06	179.99	−178.50	179.92

from a nucleophile was increased. Chemical softness (σ) characterizes an atom's propensity to accept an electron or electrons. The chemical softness of INH was increased in all molecules, which suggests an increase in reactivity upon interaction with alcohol.

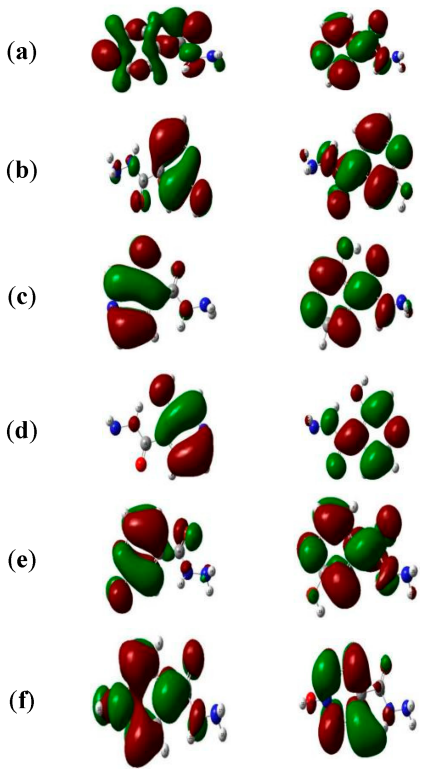

Figure 2: Orbitals involved in the electronic transition of INH (**a**), INH OH1 (**b**), INH OH2 (**c**), INH OH4 (**d**), INH OH5 (**e**) and INH OHN (**f**) for the Highest Occupied Molecular Orbital (HOMO) and Lowest Unoccupied Molecular Orbital (LUMO) respectively.

3.4. Vibrational Analysis

The infrared spectra of the studied molecules are presented in Figure 3, while the frequencies, intensities, and locations are listed in Table S1. C-C vibration occurred at 1300 cm^{-1}, 1334 cm^{-1}, 1357 cm^{-1}, 1325 cm^{-1}, 1329 cm^{-1} and 1323 cm^{-1} for INH, INHOH1, INHOH2, INHOH4, INHOH5 and INHOHN respectively. C=C stretching vibrations was observed at 1604.88 cm^{-1}, 1618.98 cm^{-1}, 1601.69 cm^{-1}, 1607.23 cm^{-1}, 1621.00 cm^{-1} and 1652.89cm^{-1} for INH, INHOH1, INHOH2, INHOH4, INHOH5 and INHOHN respectively. NH_2 bending vibrations was observed at 1686.55 cm^{-1}, 1686.55 cm^{-1}, 1683.04 cm^{-1}, 1688.49 cm^{-1}, 1685.26 cm^{-1} and 1676.35 cm^{-1} for INH, INHOH1, INHOH2, INHOH4, INHOH5 and INHOHN respectively. C=O stretching vibrations for INH was observed at 1778 91 cm^{-1} while for INHOH1, INHOH2, INHOH4, INHOH5 and INHOHN it was observed at 1777.07 cm^{-1}, 1732.58 cm^{-1}, 1769.27 cm^{-1}, 1781.81 cm^{-1}, 1732.57 cm^{-1}, respectively. C-H stretch is observed at 3171.21cm^{-1}, 3174.84 cm^{-1}, 3178.63 cm^{-1}, 3126.87 cm^{-1}, 3180.12 cm^{-1}, 3207.26 cm^{-1}, for INH, INHOH1, INHOH2, INHOH4, INHOH5 and INHOHN respectively. NH_2 symmetric stretching vibrations occurred at 3505.31 cm^{-1}, 3505.20 cm^{-1}, 3508.25 cm^{-1}, 3500.83 cm^{-1}, 3505.00 cm^{-1} and 3490.89 cm^{-1}, for INH, INHOH1, INHOH2, INHOH4, INHOH5 and INHOHN respectively. N-H stretch was observed at 3564.99 cm^{-1}, 3570.42 cm^{-1}, 3600.75 cm^{-1}, 3583.45 cm^{-1}, 3555.42 cm^{-1} and 3537.94 cm^{-1} for INH, INHOH1, INHOH2, INHOH4, INHOH5 and INHOHN respectively. NH2 asymmetric stretch was observed at 3614.16 cm^{-1}, 3612.39 cm^{-1}, 3613.64 cm^{-1}, 3601.12 cm^{-1} and 3616.01 cm^{-1}, 3616.87 cm^{-1} for INH, INHOH1, INHOH2, INHOH4, INHOH5 and INHOHN respectively. While O-H stretch was observed at 3827 37 cm^{-1}, 3291. 51 cm^{-1}, 3812.46 cm^{-1}, 3831.46 cm^{-1} and 3775.37 cm^{-1} for INHOH1, INHOH2, INHOH4, INHOH5 and INHOHN respectively.

3.5. UV-vis Spectroscopic Analysis

The UV-vis analysis was studied by TD-SCF/IEF-PCM/B3LYP 6-311+G (d,p). The resulting UV-visible spectra of the studied molecules in aqueous medium are shown in Figure 4, while the wavelengths (λ_{max}), excitation energy (E), and oscillator strengths are listed in Table S2. From our result, INH was observed to have an oscillator strength of 0.0045 and a wavelength of 279 nm, while INHOH1, INHOH2, INHOH4, INHOH5, and INHOHN had 0.0554 and 275 nm, 0.1443 and 295 nm, 0.1047 and 273 nm, 0.0636 and 274 nm, 0.0015 and 547 nm, respectively. These transitions corresponding to $\pi \rightarrow \pi^*$ transition are

Table 4: Quantum Chemical Descriptors of Studied Molecules.

	INH	INHOH1	INHOH2	INHOH4	INHOH5	INHOHN
E_{HOMO} (eV)	−0.266	−0.257	−0.246	−0.262	−0.257	−0.161
E_{LUMO} (eV)	−0.068	−0.067	−0.074	−0.071	−0.066	−0.036
ΔE_{gap} (eV)	0.198	0.190	0.171	0.195	0.191	0.131
IP (eV)	0.266	0.257	0.246	0.262	0.257	0.161
EA (eV)	0.068	0.067	0.074	0.071	0.066	0.036
μ (eV)	−0.167	−0.162	−0.160	−0.166	−0.161	−0.098
χ (eV)	0.167	0.162	0.160	0.166	0.161	0.098
η (eV)	0.099	0.095	0.086	0.096	0.095	0.063
σ (eV)	5.05	5.26	5.81	5.20	5.26	7.94
ω (eV)	0.140	0.137	0.148	0.143	0.136	0.076

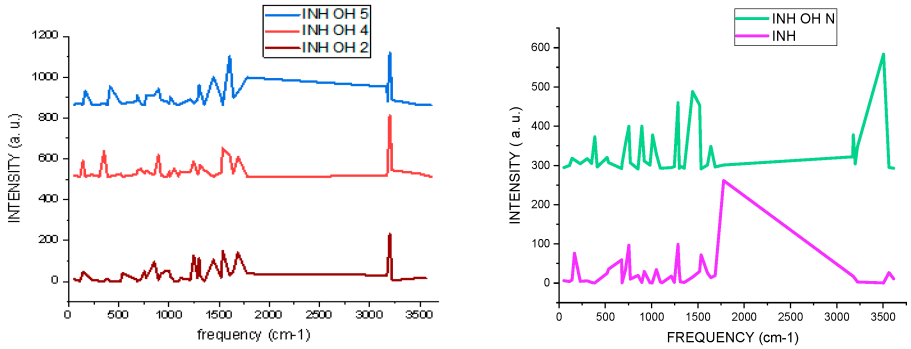

(a) (b)

Figure 3: Simulated IR spectra of studied INH molecule with -OH at Carbon 2, 4 and 5 atoms (**a**), INH molecule and INH with -OH at N atom (**b**).

governed by HOMO→LUMO excitation. From our results, we observe that the absorption wavelength of INH was extended remarkably from 278 nm to 295 nm and 547 nm in INHOH2 and INHOHN, respectively. On the other hand, it was lowered in others. The red and blue shift observed shows that the optical property of INH was altered by alcohol interaction with the N atom of the pyridyl ring and the carbon atoms of INH. These extensions increase as the band gap decreases.

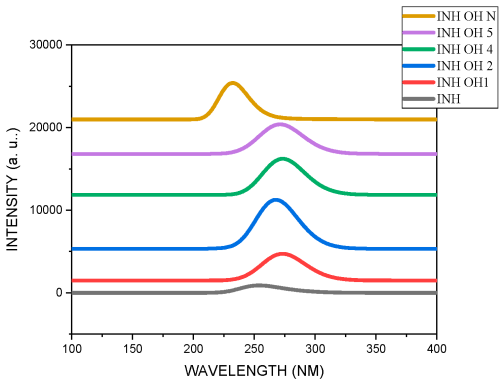

Figure 4: Simulated UV-Vis spectra of the studied molecules in water.

3.6. Natural Bonding Orbital (NBO) Analysis

Natural bond orbital (NBO) analysis is a suitable method for understanding the nature of intra- and intermolecular bonding interactions existing in bonds. It also establishes a fair ground for studying charge transfer or closed-shell interactions in molecules [43]. The greater the perturbation energy value, the stronger the interaction between the electron donors and the more the conjugation of the system [44]. The second-order perturbation energy values of INH, INHOH1, INHOH2, INHOH4, INHOH5, and INHOHN were identified from the second-order Fock matrix perturbation theory using DFT/B3LYP/6-31+G (d, p) functional. The most interacting NBOs are presented in Tables S3–S8 for INH, INHOH1, INHOH2, INHOH4, INHOH5, and INHOHN, respectively. From our result, the transition from π*-π* had a major contribution to the electron transition. Hyper intra-molecular conjugative interactions in the molecules are formed by the orbital overlap between π*C5-N6 and π*C3-C4 for INH, π*C1-N6 and π*C2-C3 for INHOH1, π*C10-O11 and π*C2-C3 for INHOH2, π*C5-N6 and π*C3-C4 for INHOH4 and INHOH5, LP (1) C3 and π*C11-O12 for INH OH1. Per-

2025, Vol. 2, Article ID. 2025.0010
https://doi.org/10.69709/MolModC.2025.112309

turbation energies of 236.93 kcal/mol, 180.40 kcal/mol, 141.83 kcal/mol, 282.82 kcal/mol, 245.78 kcal/mol, and 31.23 kcal/mol were obtained for INH, INHOH1, INHOH2, INHOH4, INHOH5, and INHOHN, respectively. This shows that donor-acceptor interaction was strongest in INHOH4 and lowest in INHOHN.

3.7. Binding Energy and Dipole Moment

The binding energies are 317. 988 kcal/mol, 315.633 kcal/mol, 321.002 kcal/mol, 319.036 kcal/mol, and 2.0877 kcal/mol were calculated for INHOH1, INHOH2, INHOH4, INHOH5, and INHOHN, respectively (Table S9). These positive binding energies suggest that alcohol binding to INH is less favourable. Dipole moments were calculated as 6.128 debye, 5.512 debye, 5.972 debye, 5.911 debye, and 4.622 debye for INHOH1, INHOH2, INHOH4, INHOH5, and INHOHN, respectively (Table S10). High binding energies, small energy gaps, and large dipole moments favour active interactions. This correlates with the narrow band gaps calculated for the molecules, which all suggest high interactions and reactivity between alcohol and isoniazid.

4. Conclusions

This research aimed to establish the possible effect of alcohol active group on the structure, molecular properties, and reactivity of isoniazid. The results suggest that the geometrical parameters (bond lengths, bond angles, and dihedral angles) of INH were slightly adjusted by the OH attached to its carbon atoms. These changes are suspected to be responsible for the overall changes observed in its properties. The C1–C2 bond length, calculated as 1.394 Å in INH, was found to be 1.403 Å, 1.412 Å, 1.391 Å, 1.392 Å, and 1.364 Å in INHOH1, INHOH2, INHOH4, INHOH5, and INHOHN, respectively.From our result, the molecules possessed small values of both the HOMO and LUMO energies, ranging between −0.26 and −0.16 and −0.07 and −0.03 eV, respectively, informing us that electrons are loosely bound. Due to a small energy gap, quick electron transfers and exchange occurred to the same degree, making these molecules very reactive. The energy gap for the studied molecules was observed in the following order: INHOHN (0.131 eV) < INHOH2 (0.171 eV) < INHOH1 (0.190 eV) < INHOH5 (0.191 eV) < INHOH4 (0.195 eV) < INH (0.198 eV). From our results, the interaction of alcohol with INH lowered its energy gap, with the lowest energy gap (0.131 eV) observed in INHOHN. This suggests that the greatest change in INH reactivity occurs when the OH group of alcohol attacks the nitrogen atom of the pyridyl ring. From our results, we observed that the absorption wavelength of INH was extended remarkably from 278 nm to 295 nm and 547 nm in INHOH2 and INHOHN, respectively. This red shift observed shows that the optical property of INH was tuned by alcohol interaction with the N atom of the pyridyl ring and the carbon atoms of INH. The binding energies are 317 Kcal/mol. 988 Kcal/mol, 315.633 kcal/mol, 321.002 kcal/mol, 319.036 kcal/mol, and 2.0877 kcal/mol were calculated for INH, INHOH1, INHOH2, INHOH4, INHOH5, and INH OHN, respectively. These positive binding energies suggest that alcohol binding to INH is less favourable. Dipole moments were calculated as 6.128 debye, 5.512 debye, 5.972 debye, 5.911 debye, and 4.622 debye for INH, INHOH1, INHOH2, INHOH4, INHOH5, and INHOHN, respectively. High binding energies, small energy gaps, and large dipole moments favour active interactions. This is in good agreement with the narrow energy gaps calculated for the molecules. These observed changes in molecular properties could be useful in understanding alcohol/isoniazid interaction, handling adverse cases in alcoholic patients, better drug administration, and new alternative drug development.

List of Abbreviations

B3LYP	Becke's Three-Parameter Exchange Functional Combined with the Lee–Yang–Parr Correlation Functional
DFT	Density Functional Theory
FMO	Frontier Molecular Orbital
HOMO	Highest Occupied Molecular Orbital
IEFPCM	Integral Equation Formalism Polarizable Continuum Model
INH	Isonicotinylhydrazine
LUMO	Lowest Unoccupied Molecular Orbital
MESP	Molecular Electrostatic Potential
NBO	Natural Bond Orbital
TDSCF	Time-Dependent Self-Consistent Field
ZPVES	Zero-point Vibrational Energies

Author Contributions

C.A.A.: Conceptualization, Methodology, Software, Validation, Investigation, Writing Original draft, Writing Review. E.A.A.: Resources, Data Curation and Editing. A.A.A.: Visualization, Supervision, and Project Administration. All authors have read and agreed to the published version of the manuscript.

Availability of Data and Materials

Data supporting the results of this study are available upon request from the corresponding author.

Consent for Publication

No consent for publication is required, as the manuscript does not involve any individual personal data, images, videos, or other materials that would necessitate consent.

Conflicts of Interest

The authors declare no conflicts of interest.

Funding

The study did not receive any external funding and was conducted using only institutional resources.

Acknowledgments

The authors would like to acknowledge the University of Calabar for providing the necessary facilities and support that enabled the successful conduct of this research.

Supplementary Materials

The supplementary materials are available at: https://doi.org/10.69709/MolModC.2025.112309.

References

[1] Argyrou, A.; Vetting, M.W.; Aladegbami, B.; Blanchard, J.S. Mycobacterium Tuberculosis Dihydrofolate Reductase Is a Target for Isoniazid. *Nat. Struct. Mol. Biol.* **2006**, *13*, 408–413. [CrossRef] [PubMed]

[2] Banerjee, A.; Dubnau, E.; Quemard, A.; Balasubramanian, V.; Um, K.S.; Wilson, T.; Collins, D.; de Lisle, G.; Jacobs, W.R., Jr. inhA, a Gene Encoding a Target for Isoniazid and Ethionamide in Mycobacterium Tuberculosis. *Science* **1994**, *263*, 227–230. [CrossRef] [PubMed]

[3] Bardou, F.; Raynaud, C.; Ramos, C.; Laneelle, M.A.; Laneelle, G. Mechanism of Isoniazid Uptake in Mycobacterium Tuberculosis. *Microbiology* **1998**, *144*, 2539–2544. [CrossRef] [PubMed]

[4] Slayden, R.A.; Barry, C.E., III. The Genetics and Biochemistry of Isoniazid Resistance in Mycobacterium Tuberculosis. *Microbes Infect.* **2000**, *2*, 659–669. [CrossRef] [PubMed]

[5] Slayden, R.A.; Lee, R.E.; Barry, C.E. III Isoniazid Affects Multiple Components of the Type II Fatty Acid Synthase System of Mycobacterium Tuberculosis. *Mol. Microbiol.* **2000**, *38*, 514–525. [CrossRef] [PubMed]

[6] Takayama, K.; Wang, L.; David, H.L. Effect of Isoniazid on the In Vivo Mycolic Acid Synthesis, Cell Growth, and Viability of Mycobacterium Tuberculosis. *Antimicrob. Agents Chemother.* **1972**, *2*, 29–35. [CrossRef] [PubMed]

[7] Ameeruddin, N.U.; Selvakumar, S.; Luke, E.H.; Nagamiah, S. Overview on Mechanisms of Isoniazid Action and Resistance in Mycobacterium Tuberculosis. *Infect. Genet. Evol.* **2016**, *45*, 474–492. [CrossRef] [PubMed]

[8] WHO. *Global Tuberculosis Report 2017*; WHO: Geneva, Switzerland, 2017; https://www.who.int/publications/i/item/9789241565516.

[9] Rehm, J.; Samokhvalov, A.V.; Neuman, M.G.; Room, R.; Parry, C.; Lönnroth, K.; Patra, J.; Poznyak, V.; Popova, S.; Brock, T.; et al. The Association Between Alcohol Use, Alcohol Use Disorders and Tuberculosis (TB). A Systematic Review. *BMC Public Health* **2009**, *9*, 450. [CrossRef] [PubMed]

[10] Volkmann, T.; Moonan, P.K.; Miramontes, R.; Oeltmann, J.E. Tuberculosis and Excess Alcohol Use in the United States 1997-2012. *Int. J. Tuberc. Lung Dis.* **2015**, *19*, 111–119. [CrossRef] [PubMed]

[11] National Institute on Alcohol Abuse and Alcoholism. cine.htm. Mixing Alcohol with Medicines. 2014. Available online: http://pubs.niaaa.nih.gov/publications/Medicine/medi (accessed on 6 November 2015).

[12] Brown, R.L.; Dimond, A.R.; Hulisz, D. Pharmacoepidemiology of Potential Alcohol-Prescription Drug Interactions Among Primary Care Patients with Alcohol-Use Disorders. *J. Am. Pharm. Assoc* **2007**, *47*, 135–139. [CrossRef] [PubMed]

[13] Jang, G.R.; Harris, R.Z. Drug Interactions Involving Ethanol and Alcoholic Beverages. *Expert Opin. Drug Metab. Toxicol.* **2007**, *3*, 719–731. [CrossRef] [PubMed]

[14] Weathermon, R.; Crabb, D.W. Alcohol and Medication Interactions. *Alcohol. Res. Health* **1999**, *23*, 40–54. [PubMed]

[15] Chan, L.N.; Anderson, G.D. Pharmacokinetic and Pharmacodynamic Drug Interactions with Ethanol (Alcohol). *Clin. Pharmacokinet.* **2014**, *53*, 1115–1136. [CrossRef] [PubMed]

[16] Fraser, A.G. Pharmacokinetic Interactions Between Alcohol and Other Drugs. *Clin. Pharmacokinet.* **1997**, *33*, 79–90. [CrossRef] [PubMed]

[17] Quertement, E.; Didone, V. Role of Acetaldehyde in Mediating the Pharmacological and Behavioral Effects of Alcohol. *J. Natl. Inst. Alcohol Abus. Alcohol.* **2006**, *29*, 258–265. https://www.researchgate.net/publication/6122486_Role_of_acetaldehyde_in_mediating_the_pharmacological_and_behavioral_effects_of_alcohol/link/53fc53620cf22f21c2f3c5aa/download?_tp=eyJjb250ZXh0Ijp7ImZpcnN0UGFnZSI6InB1YmxpY2F0aW9uIiwicGFnZSI6InB1YmxpY2F0aW9uIn19.

[18] Salaspuro, M. Microbial Metabolism of Ethanol and Acetaldehyde and Clinical Consequences. *Addict. Biol.* **2006**, *2*, 35–46. [CrossRef] [PubMed]

[19] Regby-Jones, A.E.; Sneyd, J.R. Pharmacokinetics and Pharmacodynamics—Is There Anything New? *Anaesthesia* **2012**, *67*, 5–11. [CrossRef] [PubMed]

[20] Kline, S.S.; Mauro, V.F.; Forney, R.B., Jr.; Freimer, E.H.; Somani, P. Cefotetan-Induced Disulfiram-Type Reactions and Hypoprothrombinemia. *Antimicrob.*

Agents Chemother. **1987**, *31*, 1328–1331. [CrossRef] [PubMed]

[21] Norrby, S.R. Adverse Reactions and Interactions with Newer Cephalosporin and Cephamycin Antibiotics. *Med. Toxicol.* **1986**, *1*, 32–46. [CrossRef] [PubMed]

[22] Billstein, S.A.; Sudol, T.E. Disulfiram-Like Reactions Rare with Ceftriaxone. *Geriatrics* **1992**, *47*, 70. [PubMed]

[23] Heelon, M.W.; White, M. Disulfiram-Cotrimoxazole Reaction. *Pharmacotherapy* **1998**, *18*, 869–870. [CrossRef] [PubMed]

[24] Fernandez-Villar, A.; Sopena, B.; Vazquez, R.; Ulloa, F.; Fluiters, E.; Moisteiro, M.; Martinez-Vazquez, C.; Pineiro, L. Isoniazid Hepatotoxicity Among Drug Users: The Role of Hepatitis C. *Clin. Infect. Dis.* **2003**, *36*, 293–298. [CrossRef] [PubMed]

[25] Wendel, M.W.; David, M.H. Clinical pharmacokinetics of Isoniazid. *Pharmacokinetic* **2012**, *4*, 401–433. [CrossRef]

[26] Katiyar, S.K.; Bihari, S.; Prakash, S.; Mamtani, M.; Kulkarni, H. A andomized controlled trial of high-dose isoniazid adjuvant therapy for multidrug-resistant tuberculosis. *Int. J. Tuberc. Lung Dis.* **2008**, *12*, 139–145. [PubMed]

[27] Koriakin, V.A.; Sokolova, G.B.; Grinchar, N.A.; Iurchenko, L.N. Pharmacokinetics of Isoniazid in Patients with Pulmonary Tuberculosis and Alcoholism. *Probl. Tuberk.* **1986**, *1986*, 43–46. [PubMed]

[28] Lester, D. The Acetylation of Isoniazid in Alcoholics. *Q. J. Stud. Alcohol.* **1964**, *25*, 541–543. [CrossRef] [PubMed]

[29] Wilcke, J.T.R.; Døssing, M.; Angelo, H.R.; Askgaard, D.; Rønn, A.; Christensen, H.R. Unchanged Acetylation of Isoniazid by Alcohol Intake. *Int. J. Tuberc. Lung Dis.* **2004**, *11*, 1373–1376. [PubMed]

[30] Anoop, k.P.; Abhishek, B.; Vikas, B.; Apoorva, D. Structural, Electronic, and Vibrational Properties of Isoniazid and Its Derivative N-Cyclopentylidenepyridine-4-carbohydrazide: A Quantum Chemical Study. *J. Theor. Chem. Vol.* **2014**, *2014*, 894175. [CrossRef]

[31] Hajar, S.; Nina, K.; Shahriar, G.; Farshid, S.; Kheyrollah, M. Crystal Structure and Density Functional Theory Study on Structural Properties and Energies of a Isonicotinohydrazide Compound. *Molecules* **2011**, *16*, 7715–7724. [CrossRef] [PubMed]

[32] *Gauss View*; Version 5; Ray Dennington, Todd Keith and John Milam, Semichem Inc.: Shawnee Mission, KS, USA, 2009; https://scholar.google.com/scholar?hl=en&as_sdt=0%2C5&q=Gauss+View%2C+Version+5%2C+Ray+Dennington%2C+Todd+Keith+and+John+Milam%2C+Semichem+Inc.%2C+Shawnee+Mission+KS%2C+2009&btnG=.

[33] Frisch, M.J.; Trucks, G.W.; Schlegel, H.B.; Scuseria, G.E.; Robb, M.A.; Cheeseman, J.R.; Scalmani, G.; Barone, V.; Petersson, G.A.; Nakatsuji, H.; et al. *Gaussian 09, Revision C. 02*; Gaussian, Inc.: Wallingford, CT, USA, 2009; https://scholar.google.com/scholar?hl=en&as_sdt=0%2C5&q=%5B33%5D%09Frisch%2C+M.J.%3B+Trucks%2C+G.W.%3B+Schlegel%2C+H.B.%3B+Scuseria%2C+G.E.%3B+Robb%2C+M.A.%3B+Cheeseman%2C+J.R.%3B+Scalmani%2C+G.%3B+Barone%2C+V.%3B+Petersson%2C+G.A.%3B+Nakatsuji%2C+H.%3B+et+al.+Gaussian+09%2C+Revision+C.+02%3B+Gaussian%2C+Inc.%3A+Wallingford%2C+CT%2C+USA%2C+2009&btnG=.

[34] Geerlings, P.; De Proft, F.; Langenaeker, W. Conceptual Density Functional Theory. *Chem. Revolut.* **2003**, *103*, 1793–1874. [CrossRef] [PubMed]

[35] Becke, A.D. Density Functional Exchange Energy Approximation with Correct Asymptotic Behavior. *Phys. Rev. A At. Mol. Opt. Phys.* **1988**, *38*, 3098–3100. [CrossRef] [PubMed]

[36] Lee, C.; Yang, W.; Parr, R.G. Development of the Colle-Salveti Correlation Energy Formula into a Functional of the Electron Density. *Phys. Rev. BCondens. Matter Mater. Phys.* **1988**, *37*, 785–789. [CrossRef] [PubMed]

[37] Peng, C.; Ayala, P.Y.; Schlegel, H.B. Using Redundant Internal Coordinates to Optimize Equilibrium Geometries and Transition States. *J. Comput. Chem.* **1996**, *17*, 49–56. https://schlegelgroup.wayne.edu/Pub_folder/180.pdf. [CrossRef]

[38] Davidson, E.R.; Feller, D. Basis Set Selection for Molecularcalculation. *J. Chem. Rev.* **1986**, *86*, 681–696. [CrossRef]

[39] Koopmans, T. About the Assignment of Wave Functions and Eigenvalues to the Individual Electrons of an Atom. *Physicia Pol.* **1934**, *1*, 104–113. [CrossRef]

[40] Reed, A.E.; Curtiss, L.A.; Weinhold, F. Intermolecular Interactions from a Natural Bond Orbital, Donor—Acceptor Viewpoint. *J. Chem. Revolut.* **1988**, *88*, 899–926. [CrossRef]

[41] Fleming, D.L. *Frontier Orbitals and Organic Chemical Reactions*; John Wiley & Sons: New York, NY, USA, 1976. [CrossRef]

[42] Parr, R.G.; Yang, W. Density Functional Approach to the Frontier-Electron Theory of Chemical Reactivity. *J. Am. Chem. Soc.* **1984**, *106*, 4049–4050. [CrossRef]

[43] Rubarani, P.G.; Sampath, K.S. Natural Bond Orbital (NBO) Population Analysis of 1-Azanapthalene-8-ol. *ACTA Phys. Pol. A* **2014**, *125*, 18–22. [CrossRef]

[44] Mulliken, R.S. Electronic Population Analysis on LCAO-MO Molecular Wave Functions. *J. Chem. Phys.* **1955**, *23*, 1833. [CrossRef]